1-1-1980

Neutron diffusion-nodal model in one dimensional geometry

Roy M. Ramavarapu
Iowa State University

Neutron diffusion-nodal model in one dimensional geometry

by

Roy M. Ramavarapu

A Thesis Submitted to the
Graduate Faculty in Partial Fulfillment of the
Requirements for the Degree of
MASTER OF SCIENCE

Major: Nuclear Engineering

Iowa State University
Ames, Iowa

1980

LIST OF FIGURES

LIST OF TABLES

I. INTRODUCTION

The calculation of flux profiles and spatial power distribution in a nuclear reactor is a central problem of nuclear engineering and reactor physics. These calculations are required for the solution of a broad range of design and operational problems. They necessarily involve a high degree of accuracy and considerable spatial detail. For the most part, such calculations are carried out with computer programs that utilize the finite difference approximation to the group diffusion equations. These programs imply a minimum of 20000-30000 mesh points for a two-dimensional problem and the cost of using these fine mesh computer programs is not insignificant. In addition, there are the problems of data management and data retrieval associated with the use of these programs.

On the other hand, and in general, the power distribution calculations required for in-core fuel management decision studies do not require the same spatial detail as a design verification problem. With this end in view, there has been a major effort in developing computational models that cost less to use and still yield results with a degree of accuracy satisfactory for fuel management purposes.

Typically, in a fine mesh diffusion theory program, a mesh point is located on each fuel pin of an assembly. In the latter models, the storage requirements and computer run times are considerably reduced by employing a coarse mesh and by associating a mesh point with each assembly, and thereby dividing the reactor into nodes. In

this case, the mesh spacing for the difference equations is of the order of the fuel assembly center-to-center distance; 15 to 20 cms.

II. PROPOSED OBJECTIVE AND SCOPE

In the last decade, coarse mesh and nodal methods have become increasingly popular as a thermal reactor core analysis and design calculational tool. This has been due, in part, to the ever-increasing size of thermal reactors and the economic emphasis on operational optimization, especially in the area of nuclear fuel management.

The objective of the research described in this dissertation will be to develop a 2-group, 1-dimensional coarse mesh diffusion theory model for calculating the power distribution and flux profiles in an array of PWR fuel assemblies which simulate a slab reactor.

A one-dimensional case study will be undertaken to establish the feasibility of the method and to investigate the stability and convergence criteria involved; suggestions for extending the method to higher-order dimensions will be presented.

The model will be developed with the assumption that the core symmetry line bisects the central assembly, Figure 1. The mesh spacing considered will be equal to the fuel assembly center-to-center spacing, i.e., a node will be associated with a fuel assembly.

The flux distribution over a fuel assembly will be approximated by a second-order polynomial and the polynomial coefficients for each fuel assembly will be determined by using conditions derived from diffusion theory. The flux profiles will be obtained by evaluating the polynomial at different locations within each fuel assembly.

Discrepancies in the power and flux distributions can be expected in the assemblies on or near the core-reflector interface, since these

Figure 1. Core geometry showing core nodes (fuel assemblies)

assemblies differ widely in their fast scattering and thermal absorption cross sections. This causes a steep flux gradient which a coarse mesh model cannot accurately predict. To overcome this problem, the water reflector nodes are eliminated and an albedo boundary condition will be used to determine the coefficients for the assembly on the core-reflector interface.

Also, the flux near the edge of a fuel assembly tends to increase or decrease depending on the flux in the adjacent nodes. This will be taken into account by using empirical weighting factors to obtain an intra-nodal flux matching.

Finally, the results will be compared with those obtained from a fine mesh diffusion theory program.

III. LITERATURE REVIEW

The primary objective of this study is to develop a 2-group, 1-dimensional coarse mesh diffusion theory model to obtain the flux profiles and assembly power distributions in a slab reactor core.

Extensive work has been conducted in this aspect of nuclear engineering, especially in the area of in-core fuel management. Since many shuffling iterations may be necessary to find an optimal loading pattern, considerable effort has been devoted to the development of 1-, 1.5- and 2-group coarse mesh models which can predict the radial power distribution using a few seconds of computer time. Coarse mesh calculations usually refer to those in which the mesh spacing for the difference equations is of the order of the fuel assembly center-to-center spacing in a reactor. In the 1.5-group model, the fast flux distribution is solved using diffusion theory and the thermal flux is calculated assuming zero buckling in the thermal group. This model, described by Borresen [1] and subsequently used by Stout and Robinson [2], Lin, Zolotar and Weisman [3] uses empirically obtained weighting factors for the fast and thermal groups to adjust the net current at the assembly interfaces. Their results show moderate agreement with fine mesh PDQ-7 calculations. Lin, Zolotar and Weisman [3] have extended their model to BWRs. Chitkara and Weisman [4] have described a coarse mesh, 1-group model with one mesh point per assembly.

Stout and Robinson [2] indicate that the use of albedo boundary conditions in place of the water reflector nodes can improve their results. Much of the information on the fitting of albedo values at

the core-reflector interface is proprietary and not described in the open literature; however, Becker and Celnik [5] have described one procedure.

An alternative approach is to construct a nuclear model using the nodal method. In this case, the reactor is treated as an array of nodes, each of which is a source and sink for neutrons. Neutron interchange between these nodes is treated with empirical coupling coefficients, transport-kernels and albedos which are all functions of core geometry and material properties. Steinke [6] has developed a coarse nodal method for solving the diffusion equation in its integral Greén's function operator form. Graves [7] used a two-group nodal method to evaluate reactor power distribution. The FLARE [8] program is the evolutionary starting point for several nodal computer codes. CYREP-II [9] is a PWR nodal code which uses a two-dimensional FLARE type model to calculate the power distribution and criticality factors. A recently developed PWR nodal code is CYCLOPS [10] in which the CYREP-II model was improved by including neutron transmission from corner assemblies and leakage in the axial direction by the use of an axial buckling term; CYCLOPS uses the transport kernel defined for the FLARE model. Fairly accurate results are obtained from a nodal method, although these methods do not accurately model the core baffle at the core-reflector interface [7]. Improved, but proprietary versions of nodal codes are known to exist [11] and they are believed to yield better results than the codes described in the open literature.

IV. THEORETICAL DEVELOPMENT OF THE MODEL

The general form of the 2-group diffusion equations in 1-dimensional geometry is given by

$$D_1 \frac{d^2}{dx^2} \phi_1(x) - (\Sigma_{a1} + \Sigma_R)\phi_1(x) + \frac{1}{\lambda} [(\nu\Sigma_f)_1 \phi_1(x) + (\nu\Sigma_f)_2 \phi_2(x)] = 0$$

$$D_2 \frac{d^2}{dx^2} \phi_2(x) - \Sigma_{a2}\phi_2(x) + \Sigma_R \phi_1(x) = 0 \qquad (4.1)$$

Subscripts 1 and 2 will be used to denote quantities in the fast and thermal groups, respectively and $\phi(x)$ is the flux at point x.

Consider the 1-dimensional nodal geometry, Figure 2, where node i is shown with its nearest neighboring nodes (i - 1) and (i + 1), respectively.

Equation (4.1) can be written for node i and with the x-dependence implied but not written, one has

$$D_{1i} \frac{d^2}{dx^2} \phi_{1i} - (\Sigma_{a1i} + \Sigma_{Ri})\phi_{1i} + (\nu\Sigma_f)_{1i}\phi_{1i} + (\nu\Sigma_f)_{2i}\phi_{2i} = 0$$

$$D_2 \frac{d^2}{dx^2} \phi_{2i} - \Sigma_{a2i}\phi_{2i} + \Sigma_{Ri}\phi_{1i} = 0 \qquad (4.2)$$

In Equation (4.2),

ϕ_{1i}, ϕ_{2i}: flux (at point x) in the fast and thermal groups, respectively, for node i

D_{1i}, D_{2i}: diffusion coefficients for the fast and thermal groups, respectively, for node i

Σ_{a1i}, Σ_{a2i}: absorption cross sections for the fast and thermal groups, respectively, for node i

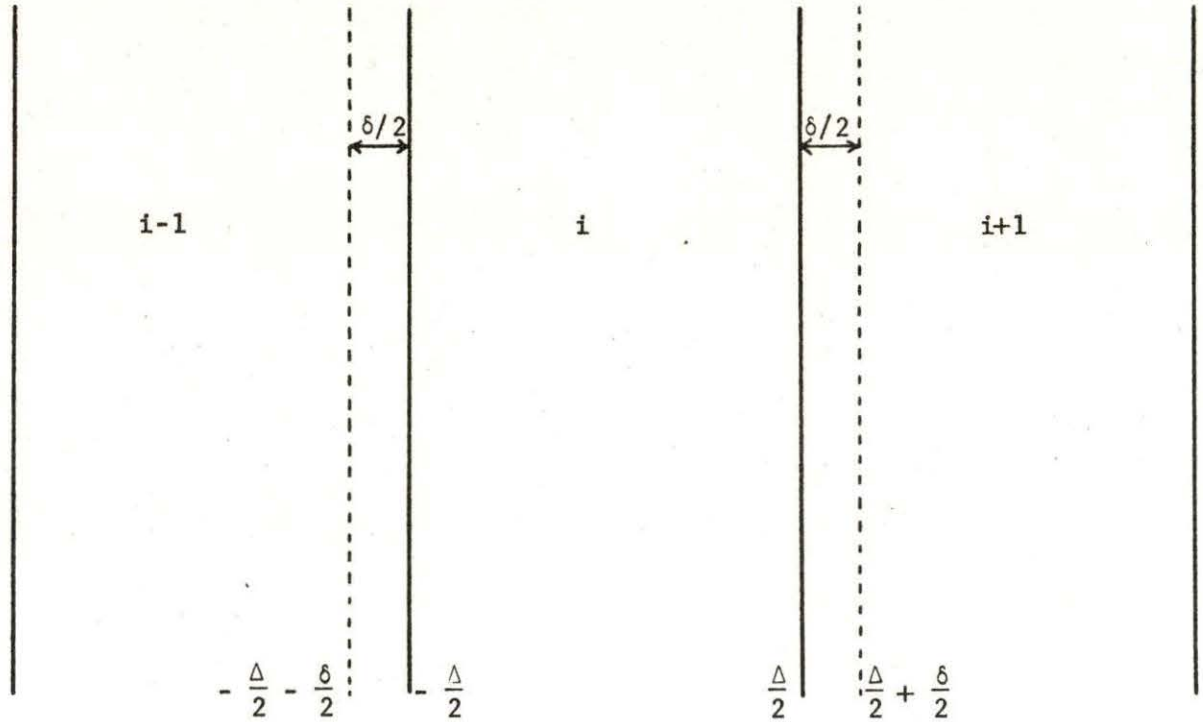

Figure 2. Geometry for flux distribution calculation

$(\nu\Sigma_f)_{1i}$, $(\nu\Sigma_f)_{2i}$: fission cross sections times the neutron yields per fission for the fast and thermal groups, respectively, for node i

Σ_{Ri}: removal cross section for the fast group in node i.

As Equation (4.2) indicates, the input to this 2-group model is simply the values of the diffusion coefficients, absorption cross sections, fission cross sections times the neutron yields per fission, the removal cross section from the fast to the thermal group for the fast and thermal groups, respectively. These seven values must be determined for each node of the problem.

For this study, the above values were obtained from the Southern California Edison Company version of the EPRI-CPM code [12]. These values were a part of the input data for the CYCLOPS nodal code.

A. Polynomial Flux Representation

The flux distribution over an assembly will be approximated by a second-order polynomial, i.e.,

$$\phi(x) = a + bx + dx^2 \tag{4.3}$$

Then the assembly averaged flux can be defined as

$$\bar{\phi} = \frac{\int \phi(x)dx}{\int dx} \tag{4.4}$$

where $\bar{\phi}$ has the same units as $\phi(x)$.

In Equation (4.3), there are three coefficients to be evaluated;

therefore, three conditions must be specified in order to evaluate these coefficients. Three conditions can be determined if one assumes that Equation (4.3) can be extended over the three regions shown in Figure 2.

A coordinate system, centered on assembly i will be used to define the function for assembly i only; however, to determine the flux coefficients it will be assumed that the flux can be extended into the surrounding assemblies, Figure 3.

Using Equations (4.3) and (4.4), the flux distributions can be integrated over the assembly i in Figure 2, i.e.,

$$\begin{aligned}
\bar{\phi}_i &= \frac{1}{\Delta}\int_{-\frac{\Delta}{2}}^{\frac{\Delta}{2}} \phi_i dx \\
\bar{\phi}^R_{\delta,i-1} &= \frac{2}{\delta}\int_{-\frac{\Delta}{2}-\frac{\delta}{2}}^{-\frac{\Delta}{2}} \phi_i dx \qquad (4.5)\\
\bar{\phi}^L_{\delta,i+1} &= \frac{2}{\delta}\int_{\frac{\Delta}{2}}^{\frac{\Delta}{2}+\frac{\delta}{2}} \phi_i dx
\end{aligned}$$

where the quantities $\bar{\phi}^R_{\delta,i-1}$ and $\bar{\phi}^L_{\delta,i+1}$ in Equation (4.5) are average fluxes in assemblies (i - 1) and (i + 1), respectively, Figure 3, i.e.,

$$\begin{aligned}
\bar{\phi}^R_{\delta,i-1} &= \frac{2}{\delta}\int_{\frac{\Delta}{2}-\frac{\delta}{2}}^{\frac{\Delta}{2}} \phi_{i-1} dx \\
&\qquad (4.6)\\
\bar{\phi}^L_{\delta,i+1} &= \frac{2}{\delta}\int_{-\frac{\Delta}{2}}^{-\frac{\Delta}{2}+\frac{\delta}{2}} \phi_{i+1} dx
\end{aligned}$$

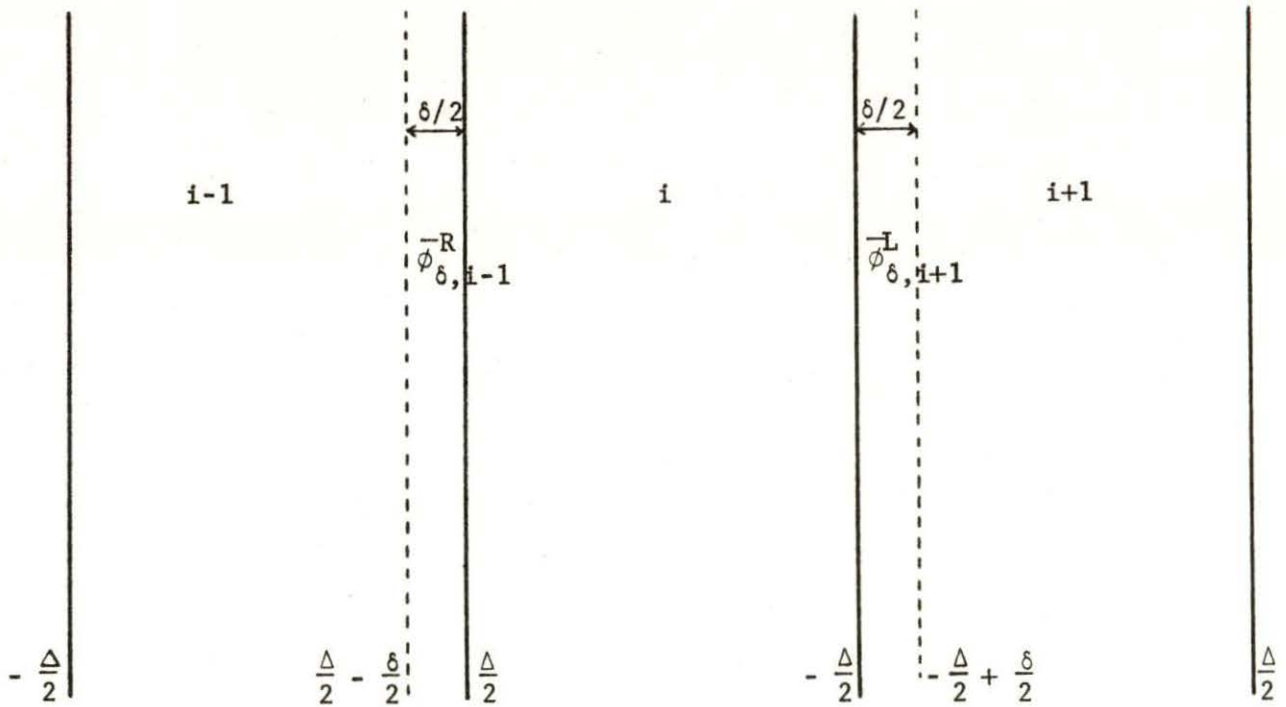

Figure 3. Geometry for partial flux calculation

and δ is a small fraction of the fuel assembly center-to-center distance Δ. Equation (4.3) can be written for assemblies (i - 1) and (i + 1), respectively, and the resulting expressions can be used in the integration of Equation (4.6), i.e.,

$$\bar{\phi}^{R}_{\delta,i-1} = a_{i-1} + b_{i-1}\left(\frac{Q}{P}\right) + d_{i-1}\left(\frac{R}{P}\right)$$

$$\bar{\phi}^{L}_{\delta,i+1} = a_{i+1} - b_{i+1}\left(\frac{Q}{P}\right) + d_{i+1}\left(\frac{R}{P}\right) \qquad (4.7)$$

where

$$P = \frac{\delta}{2}$$

$$Q = \frac{\Delta\delta}{4} - \frac{\delta^2}{8} \qquad (4.8)$$

$$R = \frac{\Delta^2\delta}{8} - \frac{\Delta\delta^2}{8} + \frac{\delta^3}{24}$$

In a similar way, Equation (4.3) can be used to integrate and solve for the unknown coefficients in Equation (4.5), i.e.,

$$a_i = \frac{P}{2(AP - C)}\left\{A(\bar{\phi}^{R}_{\delta,i-1} + \bar{\phi}^{L}_{\delta,i+1}) - \frac{2C}{P}\,(\bar{\phi}_i)\right\}$$

$$b_i = \frac{P}{2B}\left\{\bar{\phi}^{L}_{\delta,i+1} - \bar{\phi}^{R}_{\delta,i-1}\right\}$$

$$d_i = \frac{P}{2(AP - C)}\left\{2\bar{\phi}_i - (\bar{\phi}^{R}_{\delta,i-1} + \bar{\phi}^{L}_{\delta,i+1})\right\} \qquad (4.9)$$

where

$$A = \frac{\Delta^2}{12}$$

$$B = \frac{\Delta\delta}{4} + \frac{\delta^2}{8} \qquad (4.10)$$

$$C = \frac{\Delta^2\delta}{8} + \frac{\Delta\delta^2}{8} + \frac{\delta^3}{24}$$

Equations (4.7) and (4.9) can be used to evaluate the flux coefficients for any assembly not on the core-reflector interface. By using core symmetry on the central assembly, the 'δ-regions' on the right side of the central assembly can be superposed on its left, Figure 1. With this symmetry condition, the flux coefficients for the central assembly can be determined with $\bar{\phi}^{R}_{\delta,i-1} = \bar{\phi}^{L}_{\delta,i+1}$ in Equations (4.7) and (4.9).

The assembly on the core-reflector interface is treated with an albedo boundary condition and will be described in a later section.

B. Assembly Average Fluxes

To derive an expression for the average flux in an assembly, Equation (4.2) is integrated over assembly i of Figure 2, i.e.,

$$\int_{-\frac{\Delta}{2}}^{\frac{\Delta}{2}} dx[D_{1i} \frac{d^2}{dx^2} \phi_{1i} - (\Sigma_{a1i} + \Sigma_{Ri})\phi_{1i} + (\nu\Sigma_f)_{1i}\phi_{1i} + (\nu\Sigma_f)_{2i}\phi_{2i}] = 0$$

$$\int_{-\frac{\Delta}{2}}^{\frac{\Delta}{2}} dx[D_{2i} \frac{d^2}{dx^2} \phi_{2i} - \Sigma_{a2i}\phi_{2i} + \Sigma_{Ri}\phi_{1i}] = 0 \qquad (4.11)$$

If the material composition of a fuel assembly is considered homogeneous, Equation (4.11) yields

$$D_{1i}\int_{-\frac{\Delta}{2}}^{\frac{\Delta}{2}}\frac{d^2}{dx^2}\phi_{1i}dx - (\Sigma_{a1i}+\Sigma_{Ri})\int_{-\frac{\Delta}{2}}^{\frac{\Delta}{2}}\phi_{1i}dx + (\nu\Sigma_f)_{1i}\int_{-\frac{\Delta}{2}}^{\frac{\Delta}{2}}\phi_{1i}dx + (\nu\Sigma_f)_{2i}\int_{-\frac{\Delta}{2}}^{\frac{\Delta}{2}}\phi_{2i}dx = 0$$

$$D_{2i}\int_{-\frac{\Delta}{2}}^{\frac{\Delta}{2}}\frac{d^2}{dx^2}\phi_{2i}dx - \Sigma_{a2i}\int_{-\frac{\Delta}{2}}^{\frac{\Delta}{2}}\phi_{2i}dx + \Sigma_{Ri}\int_{-\frac{\Delta}{2}}^{\frac{\Delta}{2}}\phi_{1i}dx = 0 \qquad (4.12)$$

Integrating Equation (4.12) over assembly i, Figure 2 and using Equation (4.4) yields

$$\frac{D_{1i}}{\Delta}\int_{-\frac{\Delta}{2}}^{\frac{\Delta}{2}}\frac{d^2}{dx^2}\phi_{1i}dx - (\Sigma_{a1i}+\Sigma_{Ri})\bar{\phi}_{1i} + (\nu\Sigma_f)_{1i}\bar{\phi}_{1i} + (\nu\Sigma_f)_{2i}\bar{\phi}_{2i} = 0$$

$$\frac{D_{2i}}{\Delta}\int_{-\frac{\Delta}{2}}^{\frac{\Delta}{2}}\frac{d^2}{dx^2}\phi_{2i}dx - \Sigma_{a2i}\bar{\phi}_{2i} + \Sigma_{Ri}\bar{\phi}_{1i} = 0 \qquad (4.13)$$

To integrate the leakage terms of Equation (4.13), consider the reactor equation

$$\frac{d^2}{dx^2}\phi(x) = -B^2\phi(x) \qquad (4.14)$$

Since the reactor core has been decomposed into large size nodes, in which the material composition and flux are assumed uniform then, as a first approximation, Equation (4.14) can be extended to any

assembly i, i.e.,

$$\frac{d^2}{dx^2}\phi_i = - B_i^2\phi_i \tag{4.15}$$

where B_i^2 (the group notation is implied but not written) is now the average radial buckling in assembly i.

Using Equation (4.4), the above relation can be integrated over assembly i, Figure 2, i.e.,

$$\frac{1}{\Delta}\int_{-\frac{\Delta}{2}}^{\frac{\Delta}{2}} \frac{d^2}{dx^2}\phi_i dx = - B_i^2\bar{\phi}_i \tag{4.16}$$

Equation (4.16) may now be used for the leakage terms in Equation (4.13), i.e.,

$$\begin{aligned} &- D_{1i}B_{1i}^2\bar{\phi}_{1i} - (\Sigma_{a1i} + \Sigma_{Ri})\bar{\phi}_{1i} + (\nu\Sigma_f)_{1i}\bar{\phi}_{1i} + (\nu\Sigma_f)_{2i}\bar{\phi}_{2i} = 0 \\ &- D_{2i}B_{2i}^2\bar{\phi}_{2i} - \Sigma_{a2i}\bar{\phi}_{2i} + \Sigma_{Ri}\bar{\phi}_{1i} = 0 \end{aligned} \tag{4.17}$$

If one defines the assembly fission source

$$S_i \equiv (\nu\Sigma_f)_{1i}\bar{\phi}_{1i} + (\nu\Sigma_f)_{2i}\bar{\phi}_{2i} \tag{4.18}$$

and the core eigenvalue

$$\lambda \equiv \frac{\text{neutron sources}}{\text{neutron losses}}$$

then Equation (4.17) yields

$$\begin{aligned} &- D_{1i}B_{1i}^2\bar{\phi}_{1i} - (\Sigma_{a1i}+\Sigma_{Ri})\bar{\phi}_{1i} + \frac{1}{\lambda}S_i = 0 \\ &- D_{2i}B_{2i}^2\bar{\phi}_{2i} - \Sigma_{a2i}\bar{\phi}_{2i} + \Sigma_{Ri}\bar{\phi}_{1i} = 0 \end{aligned} \tag{4.19}$$

where the fission source has been multiplied by $\frac{1}{\lambda}$ to retain neutron balance.

Equation (4.19) can now be solved for the average fluxes in any assembly i, i.e.,

$$\bar{\phi}_{1i} = \frac{S_i}{D_{1i}B_{1i}^2 + (\Sigma_{a1i} + \Sigma_{Ri})}$$

$$\bar{\phi}_{2i} = \frac{\Sigma_{Ri}}{D_{2i}B_{2i}^2 + \Sigma_{a2i}} \bar{\phi}_{1i} \tag{4.20}$$

C. Assembly Average Bucklings

To evaluate the assembly average bucklings in Equation (4.20), a coordinate system centered on each assembly is used, Figure 4. Equation (4.16) can be integrated by using Equations (4.3) and (4.4), i.e.,

$$- B_i^2 \cdot \Delta \cdot (a_i + d_i \cdot A) = \frac{d}{dx} \phi_i \Big|_{\frac{\Delta}{2}} - \frac{d}{dx} \phi_i \Big|_{-\frac{\Delta}{2}} \tag{4.21}$$

Because of the polynomial approximation for the assembly flux and the assumption that Equation (4.3) can be extended into the surrounding assemblies, continuity of neutron currents at the interfaces of assemblies (i - 1), i and i, (i + 1) respectively will not be preserved, i.e.,

$$D_{i-1} \frac{d}{dx} \phi_{i-1} \Big|_{\frac{\Delta}{2}} \neq D_i \frac{d}{dx} \phi_i \Big|_{-\frac{\Delta}{2}}$$

$$D_i \frac{d}{dx} \phi_i \Big|_{\frac{\Delta}{2}} \neq D_{i+1} \frac{d}{dx} \phi_{i+1} \Big|_{-\frac{\Delta}{2}} \tag{4.22}$$

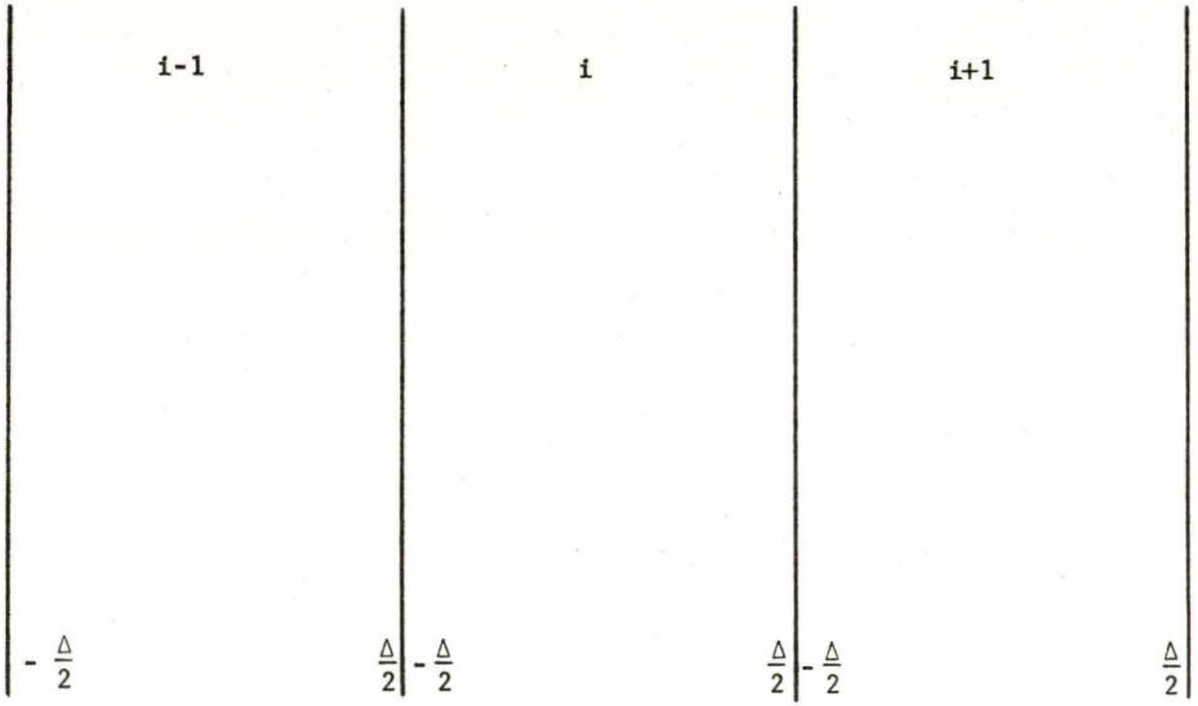

Figure 4. Geometry for evaluating assembly buckling

However, empirical weighting factors will be used to preserve continuity of neutron currents at the assembly interfaces. To do this, Equation (4.21) can be expressed as a net current by multiplying with D_i, the diffusion coefficients in node i, i.e.,

$$- B_i^2 \cdot D_i \cdot \Delta(a_i + d_i \cdot A) = D_i \frac{d}{dx} \phi_i \Big|_{\frac{\Delta}{2}} - D_i \frac{d}{dx} \phi_i \Big|_{-\frac{\Delta}{2}} \quad (4.23)$$

Then the net current across the interface between assemblies (i + 1) and i is now expressed as a weighted average of the currents at the interface between these assemblies, i.e.,

$$D_i \frac{d}{dx} \phi_i \Big|_{\frac{\Delta}{2}} = \frac{W_1' D_i \frac{d}{dx} \phi_i \Big|_{\frac{\Delta}{2}} + W_2' D_{i+1} \frac{d}{dx} \phi_{i+1} \Big|_{-\frac{\Delta}{2}}}{W_1' + W_2'} \quad (4.24)$$

where W_1', W_2' are empirical weighting factors. Equation (4.3) can be used to evaluate the above expression, i.e.,

$$D_i \frac{d}{dx} \phi_i \Big|_{\frac{\Delta}{2}} = \frac{W_1' D_i (b_i + d_i \Delta) + W_2' D_{i+1} (b_{i+1} - d_{i+1} \Delta)}{W_1' + W_2'} = J^R \quad (4.25)$$

In a similar way, the net current across the interface between assemblies (i - 1) and i can be expressed as a weighted average of the currents at the interface between these assemblies, i.e.,

$$D_i \frac{d}{dx} \phi_i \Big|_{-\frac{\Delta}{2}} = \frac{W_1 D_{i-1} (b_{i-1} + d_{i-1} \Delta) + W_2 D_i (b_i - d_i \Delta)}{W_1 + W_2} = J^L \quad (4.26)$$

where W_1, W_2 is another set of empirical weighting factors.

Equations (4.25) and (4.26) can now be used in Equation (4.23) to

estimate the buckling, i.e.,

$$B_i^2 = \frac{-1}{D_i \Delta (a_i + d_i A)} (J^R - J^L) \tag{4.27}$$

D. The Albedo Model

The detailed solution of the diffusion equations in the water reflector nodes is replaced by an equivalent albedo boundary condition at the core-reflector interface. For this analysis, the albedo, α is defined as the ratio between the neutron current out of the reflecting region to the neutron current into the reflecting region [13].

For the coordinate system centered on the end assembly, Figure 5, the effective boundary condition [13] on the flux in the region $x < \frac{\Delta}{2}$ is given by

$$\frac{1}{\phi_i} D_i \frac{d}{dx} \phi_i \Big|_{\frac{\Delta}{2}} = -0.5\left(\frac{1-\alpha}{1+\alpha}\right) = \tau \tag{4.28}$$

Using Equation (4.3) in the above relation, evaluating at the core-reflector interface and simplifying, one has

$$D_i(b_i + d_i \Delta) = \tau\left(a_i + b_i \frac{\Delta}{2} + d_i \frac{\Delta^2}{4}\right) \tag{4.29}$$

With Equation (4.29) and the first two expressions in Equation (4.5), one can solve for the flux coefficients in the end assembly. They are found in the form

$$a_i = \frac{(APG)\bar{\phi}^R_{\delta,i-1} - (BH + CG)\bar{\phi}_i}{A(PG + B) - (BH + CG)}$$

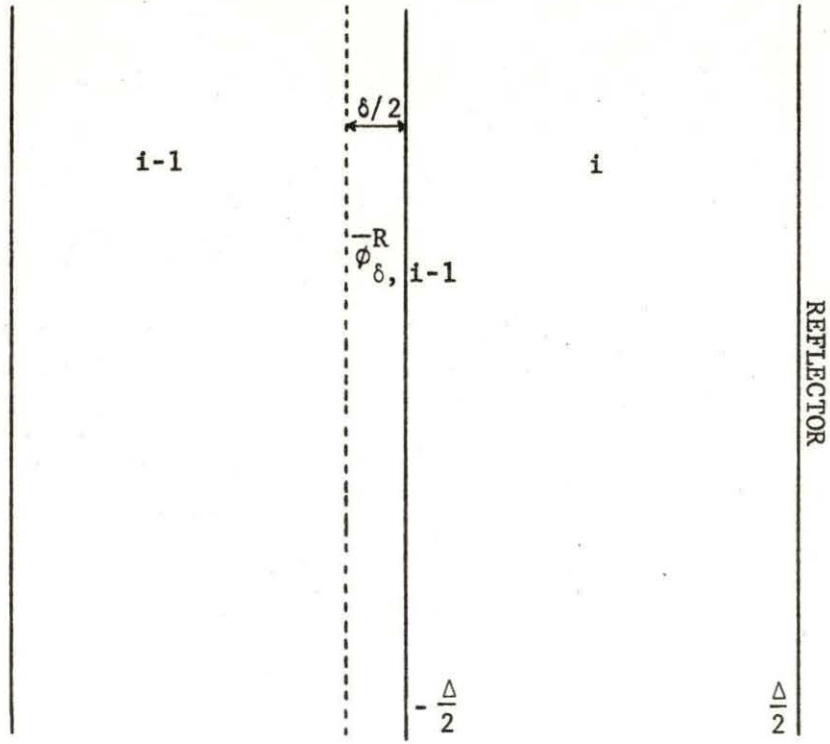

Figure 5. Geometry for albedo model for end assembly

$$b_i = \frac{(HP - AP)\bar{\phi}^R_{\delta,i-1} - (HP - C)\bar{\phi}_i}{A(PG + B) - (BH + CG)}$$

$$d_i = \frac{(GP + B)\bar{\phi}_i - (GP)\bar{\phi}^R_{\delta,i-1}}{A(PG + B) - (BH + CG)} \tag{4.30}$$

where

$$G = \frac{\Delta}{2} - \frac{D_i}{\tau}$$

$$H = \frac{\Delta^2}{4} - \frac{\Delta D_i}{\tau} \tag{4.31}$$

Equations (4.28) with Equation (4.29) can now be used to solve for the flux coefficients in the end assembly.

To determine the buckling in the end assembly, the same procedure, described earlier is adopted, except that Equation (4.28) is now written as

$$D_i \frac{d}{dx} \phi_i \Big|_{\frac{\Delta}{2}} = \tau \phi_i \Big|_{\frac{\Delta}{2}} \tag{4.32}$$

Using Equation (4.3), the above expression can be evaluated at the core-reflector interface, i.e.,

$$D_i \frac{d}{dx} \phi_i \Big|_{\frac{\Delta}{2}} = \tau(a_i + b_i \frac{\Delta}{2} + d_i \frac{\Delta^2}{4}) = J^E \tag{4.33}$$

Equation (4.31) can now be used in Equation (4.27) to evaluate the buckling in the end assembly, i.e.,

$$B_i^2 = \frac{-1}{D_i \Delta(a_i + d_i \frac{\Delta^2}{12})} (J^E - J^L) \tag{4.34}$$

V. COMPUTATIONAL PROCEDURE

The overall calculation process is illustrated in Figure 6.

An iterative technique is adopted to obtain the flux profiles and power distribution.

Computations begin by assuming an initial fission source guess, Equation (4.18); and the assembly fluxes are computed by using Equation (4.20). At each stage of the iteration process, the fission sources and fluxes are normalized over the core volume and the normalized fluxes used to evaluate an improved fission source distribution. The normalized fluxes are also used in Equations (4.7), (4.9) and (4.28) to compute the flux polynomial coefficients. The coefficients are in turn used to evaluate the assembly bucklings in Equations (4.27) and (4.32).

The iterative procedure is continued until the fission sources and assembly fluxes do not change by more than a preset tolerance limit. For faster convergence, the normalized fluxes are overrelaxed after each iteration with the exception of the first, by using the relation

$$\bar{\phi}^{\nu} = \bar{\phi}^{\nu-1} + \omega(\bar{\phi}^{\nu} - \bar{\phi}^{\nu-1})$$

where ν = iteration index

ω = overrelaxation parameter.

The iterative procedure is stopped when the fission sources and flux distributions satisfy the convergence criteria. The flux profiles are then obtained by evaluating the flux polynomial, Equation (4.3) at specific locations in each assembly and the assembly power is calculated using the relation

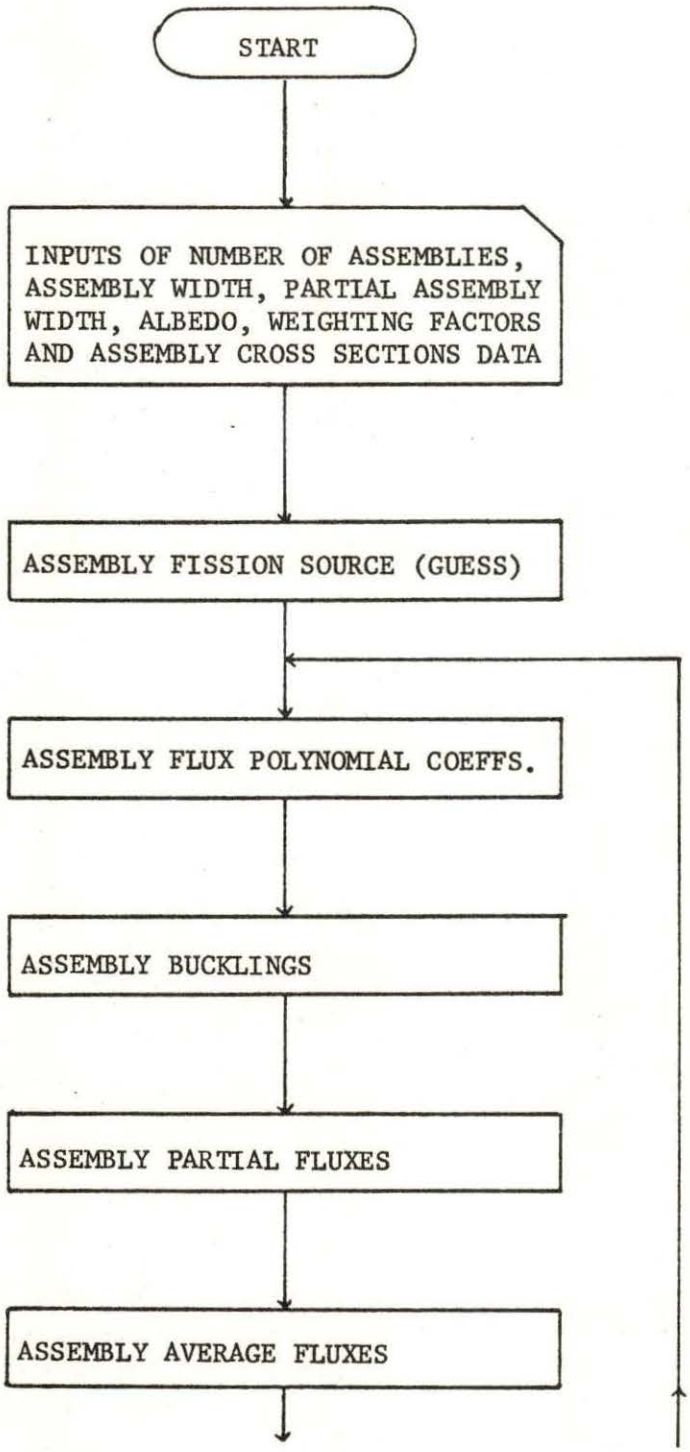

Figure 6. Flow logic for computational procedure

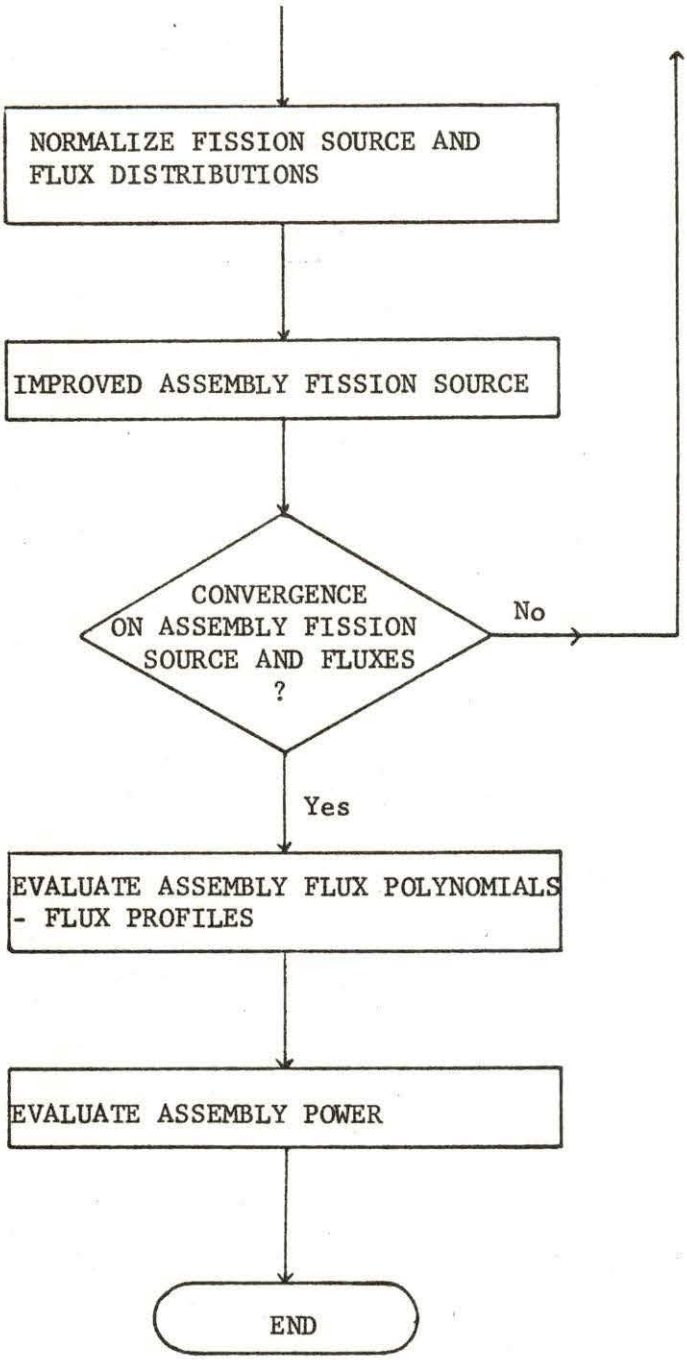

Figure 6. Continued

$$P_i = (k\Sigma_f)_{1i}\bar{\phi}_{1i} + (k\Sigma_f)_{2i}\bar{\phi}_{2i}$$

where $(k\Sigma_f)_{1i}$ and $(k\Sigma_f)_{2i}$ are the fission cross sections times the energy yields per fission for the fast and thermal groups, respectively for node i.

VI. TESTS AND RESULTS

The validity and feasibility of the coarse mesh model developed in the preceding chapters was checked by using a fine mesh, 2-group diffusion theory program, DODMG [14] as a reference calculation.

The one-dimensional slab reactor core used in this study consisted of nine PWR fuel assemblies, each 20 cms in width. The partial width δ was equal to 4 cms and the value of the albedo at the core-reflector interface was set equal to 0.3 in all the test cases.

The cross section data input to the model was obtained from the EPRI-CPM code [12]. For illustrative purposes, the input data and fuel type identification according to weight percent enrichment and number of burnable poison pins for the beginning of core life (BOL) case are listed in Table 1. The same data were used in the fine mesh reference calculations.

The fast and thermal flux profiles obtained from the coarse mesh model for the three cases of beginning of core life (BOL), middle of core life (MOL) and end of core life (EOL) are compared, in each case with those obtained from the fine mesh reference calculations. The results are illustrated in Figures 7-12 and show good agreement with the fine mesh calculations.

The model was also used to evaluate the assembly power distributions in all three cases and were found to agree reasonably well with the fine mesh calculations. These results are illustrated in Tables 2-4. The percent error between the two calculations is defined as

Table 1. Two-group EPRI-CPM data for fuel assemblies at beginning of core life (BOL)

Fuel type ID (BPP)[a]	Enrichment (wt. percent)	D(cms)	Σ_a(cm^{-1})	Σ_R(cm^{-1})	$\nu\Sigma_f$(cm^{-1})	$\kappa\Sigma_f$(cm^{-1})
A (16)	2.38	0.12744E + 01	0.94204E - 02	0.17263E - 01	0.53441E - 02	0.67386E - 13
		0.37814E + 00	0.93235E - 01	0.00	0.98190E - 01	0.12910E - 11
B (12)	2.88	0.12574E + 01	0.94461E - 02	0.17261E - 01	0.61220E - 02	0.77687E - 13
		0.38252E + 00	0.95448E - 01	0.00	0.11632E + 00	0.15319E - 11
C (0)	1.87	0.12577E + 01	0.87667E - 02	0.17857E - 01	0.49878E - 02	0.62439E - 13
		0.38112E + 00	0.71844E - 01	0.00	0.85144E - 01	0.11179E - 11

Core loading: C B C B C B C B A

[a]BPP: burnable poison pins.

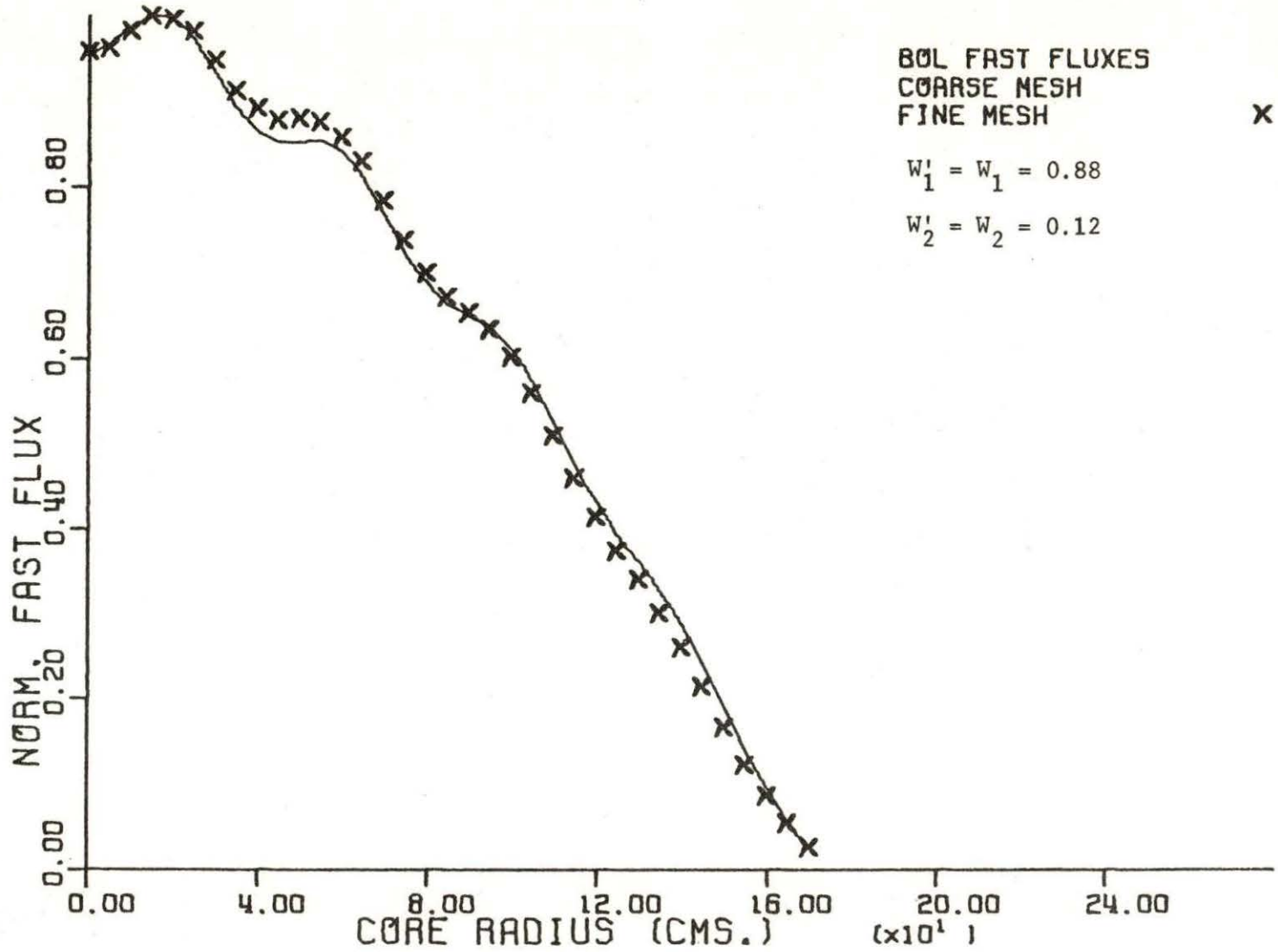

Figure 7. Comparison of fine and coarse mesh calculations. Fast flux profiles at beginning of core life

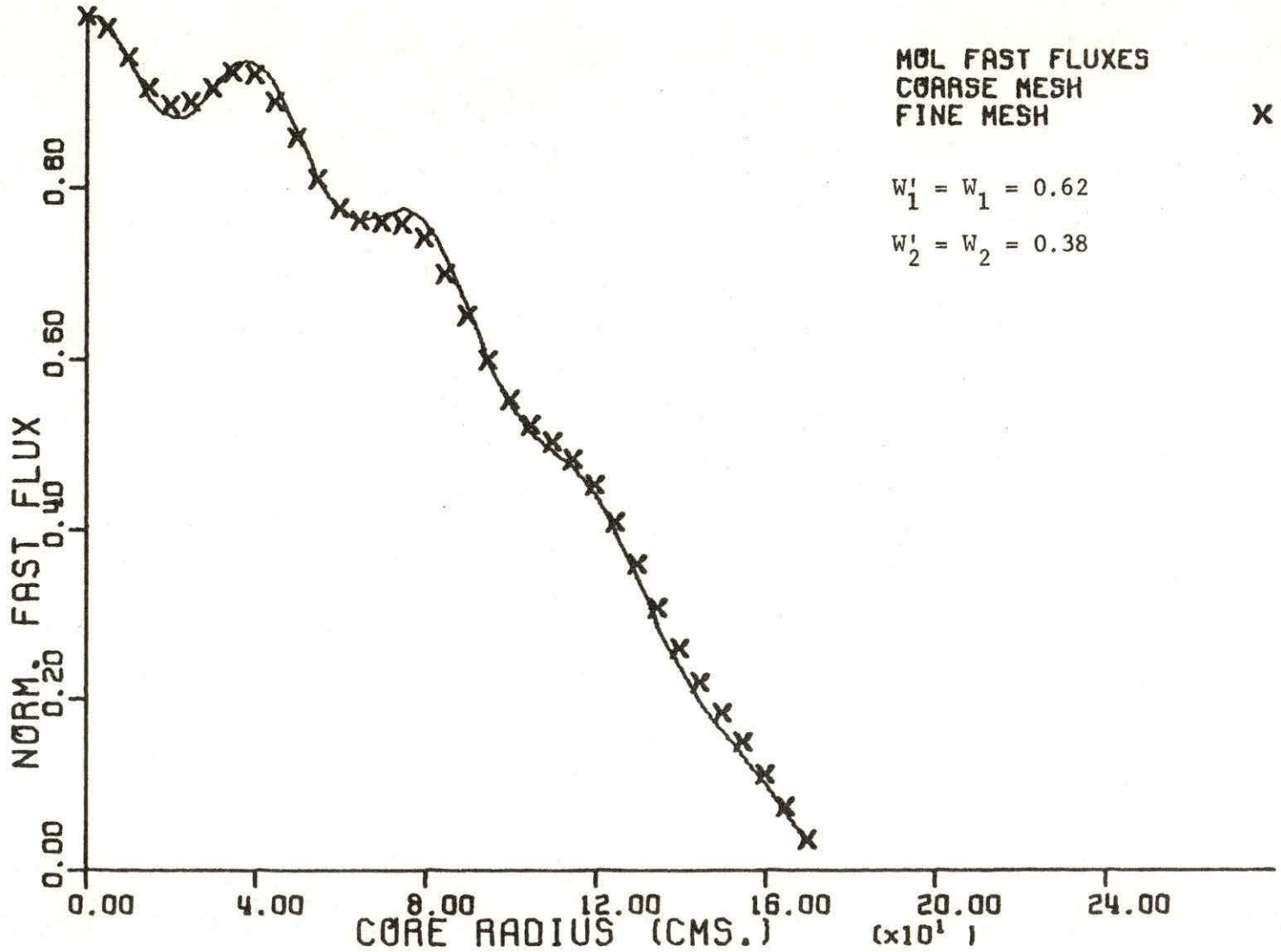

Figure 8. Comparison of fine and coarse mesh calculations. Fast flux profiles at middle of core life

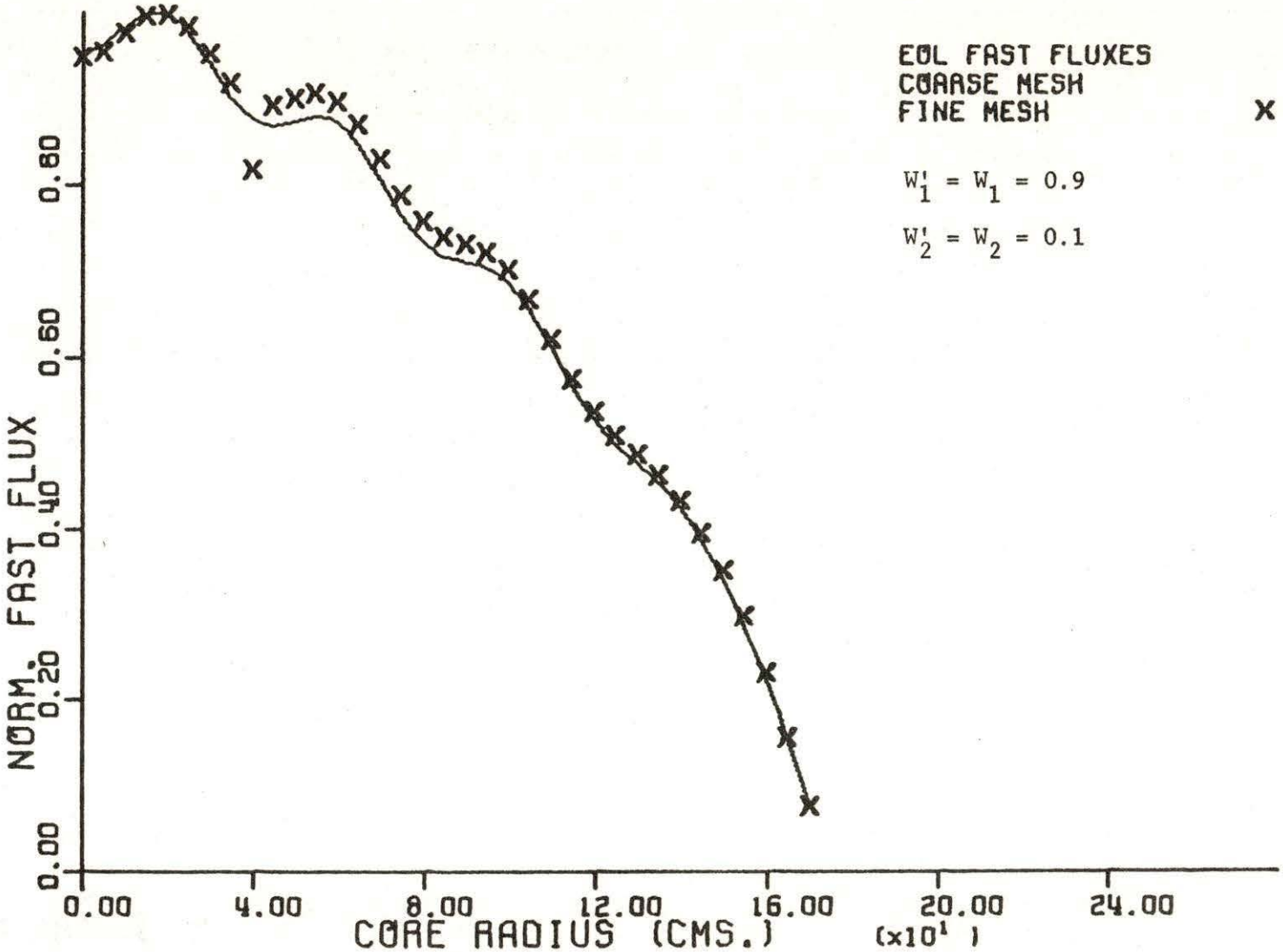

Figure 9. Comparison of fine and coarse mesh calculations. Fast flux profiles at end of core life

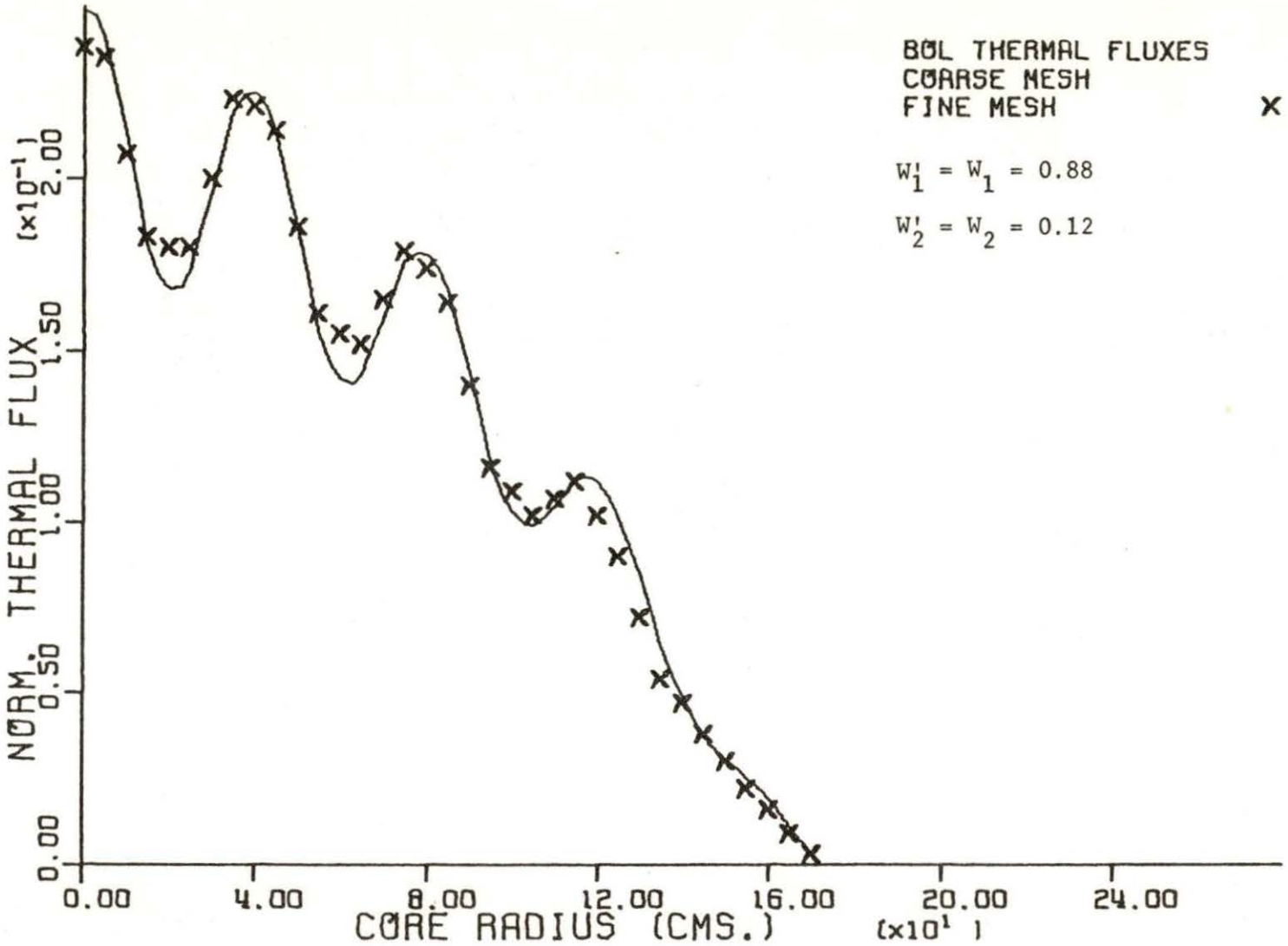

Figure 10. Comparison of fine and coarse mesh calculations. Thermal flux profiles at beginning of core life

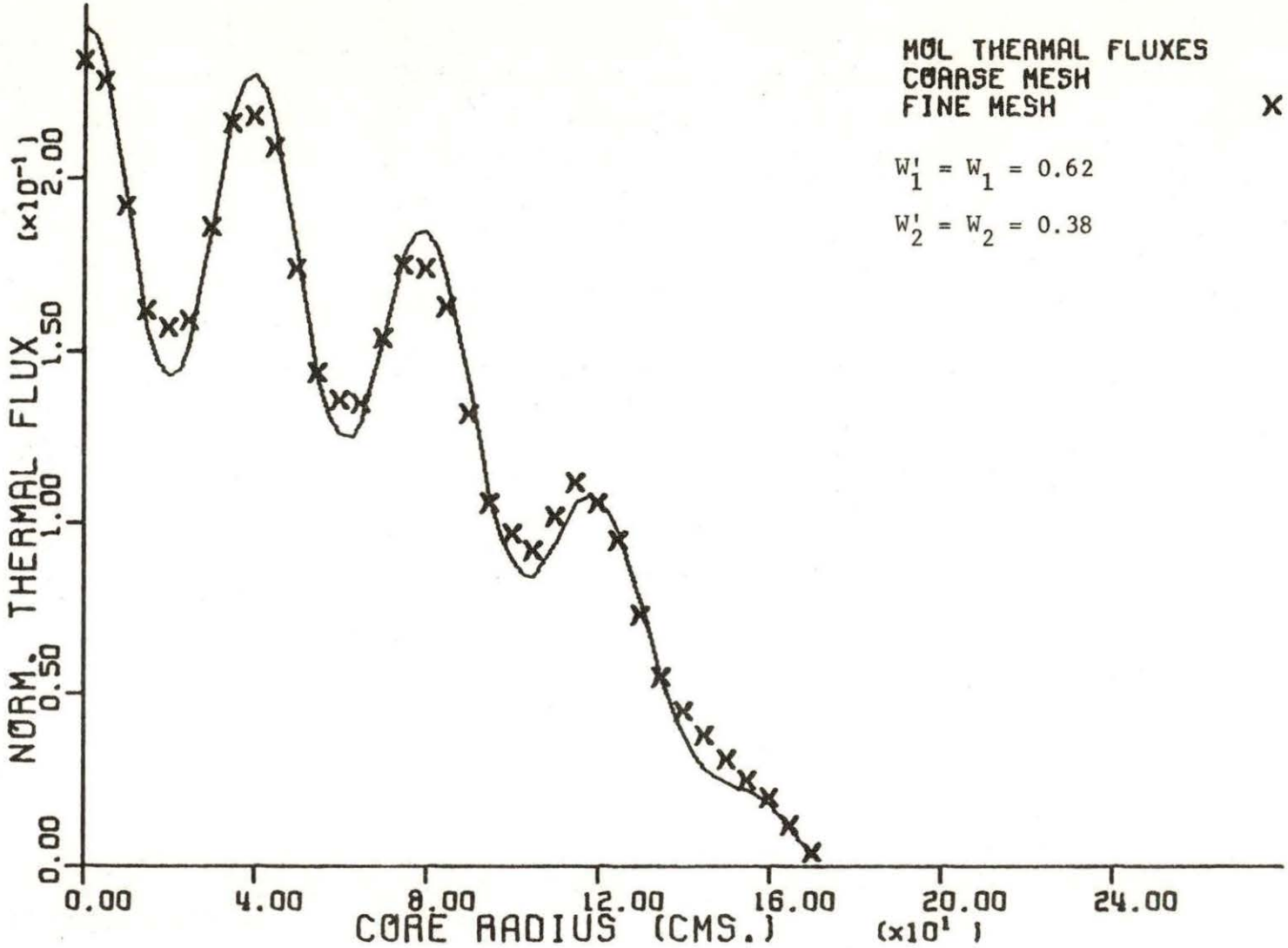

Figure 11. Comparison of fine and coarse mesh calculations. Thermal flux profiles at middle of core life

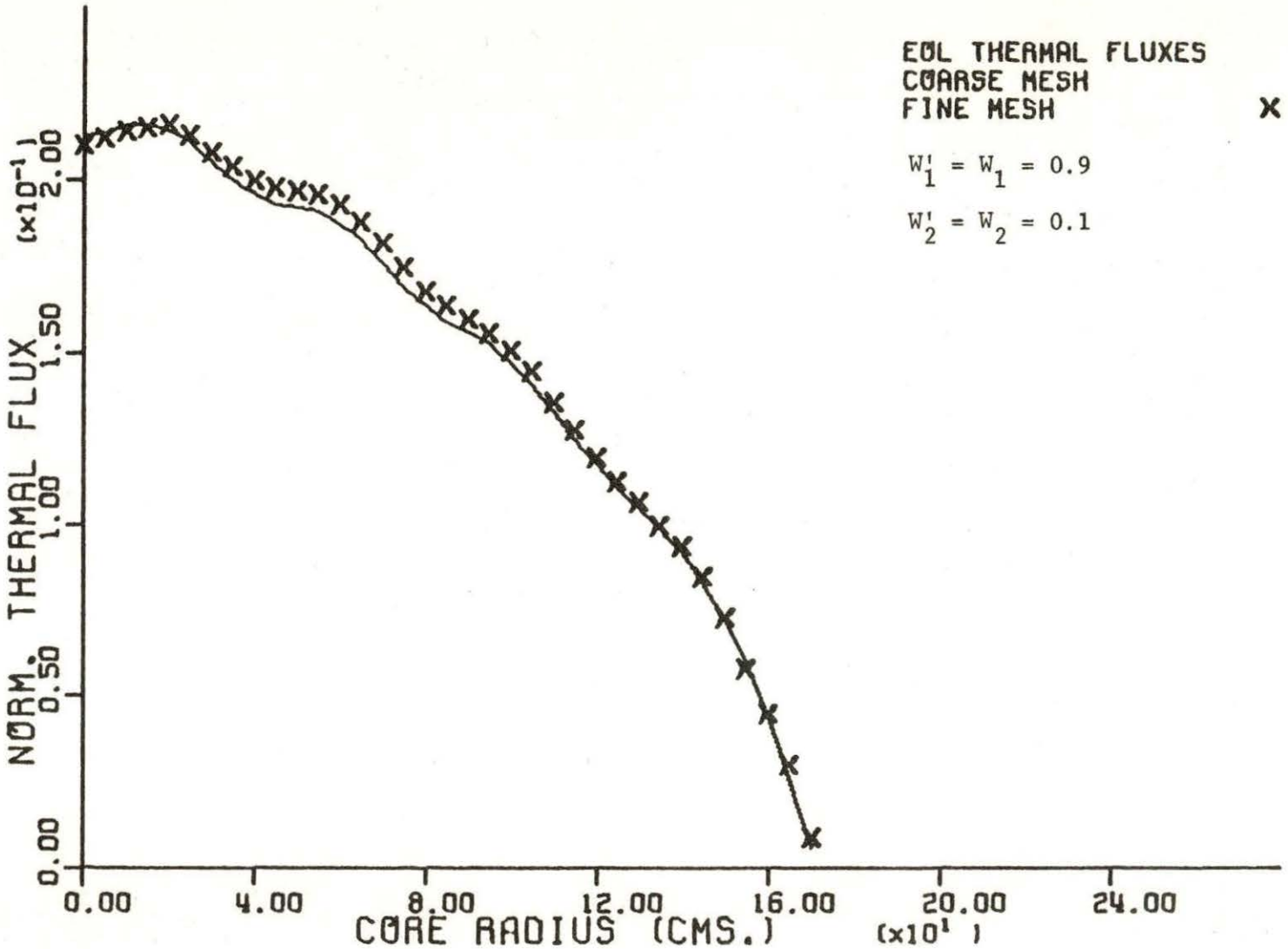

Figure 12. Comparison of fine and coarse mesh calculations. Thermal flux profiles at end of core life

Table 2. Comparison of fine and coarse mesh calculations. Power distributions at beginning of core life (BOL)

Fine mesh	1.4775	1.6354	1.3740	1.4355	1.0813	1.0057	0.6387	0.4335	0.1271
Coarse mesh	1.4548	1.5917	1.3256	1.3448	1.0529	0.9759	0.6596	0.4578	0.1367
% error	+1.54	+2.67	+3.52	+6.32	+2.63	+3.00	-3.27	-5.61	-7.55

Table 3. Comparison of fine and coarse mesh calculations. Power distributions at middle of core life (MOL)

Fine mesh	1.6362	1.4451	1.5250	1.2534	1.2142	0.8957	0.7434	0.4163	0.1888
Coarse mesh	1.6675	1.3626	1.5238	1.1972	1.2234	0.8461	0.7122	0.3659	0.1614
% error	-1.91	+5.71	+0.08	+4.48	-0.76	+5.54	+4.20	+12.11	+14.51

Table 4. Comparison of fine and coarse mesh calculations. Power distributions at end of core life (EOL)

Fine mesh	1.3241	1.4563	1.2563	1.3071	1.0596	1.0234	0.7537	0.6315	0.3502
Coarse mesh	1.3260	1.4524	1.2294	1.2694	1.0283	0.9993	0.7392	0.6180	0.3380
% error	-0.14	+0.27	+2.14	+2.88	+2.95	+2.35	+1.92	+2.14	+3.48

$$\% \text{ error} = \frac{\text{Fine mesh - Model}}{\text{Fine mesh}} \times 100$$

and is also indicated in Tables 2-4.

It is seen that there is good agreement as regards the flux profiles, especially in the case of fast flux for all three cases. The thermal flux profiles are more difficult to simulate by using a coarse mesh model due to the varying thermal absorption cross section in the reactor core. This can be seen in Figures 10 and 11 where the model cannot accurately simulate the strongly varying thermal flux behavior in the core interior. In the EOL case, Figure 12, the thermal flux is less strongly varying and there is reasonably good agreement between the two calculations.

It was found that the partial width δ had an effect on the performance of the model. The number of iterations required for convergence increased as δ increased and large values of δ also yielded less intranodal flux matching at the fuel assembly interfaces. The value of δ equal to 4 cms was taken as a limiting value; below this value the model developed numerical instabilities.

The model was also found to be dependent on the choice of weighting factors. The weighting factors that gave the best agreement with the fine mesh calculations were obtained by a trial-and-error method. This procedure required a prior knowledge of the flux profiles and was obtained from the fine mesh calculations. The optimum weighting factors are indicated in Figures 7-12. It was also found that for a given set of weighting factors, the error difference between two successive iterations was oscillatory at first, decreased rapidly and then became stable.

The assembly power distributions obtained from the fine and coarse mesh calculations are compared in Tables 2-4. It is seen that there is reasonably good agreement (on an average, within 5% of the fine mesh value) between the two calculations except for the assemblies near the core-reflector interface. The large discrepancies can be attributed to the uncertainty in the value of the albedo used in the boundary condition at the core-reflector interface.

VII. SUMMARY AND CONCLUSIONS

The coarse mesh model developed in this research has proven to be effective in simulating the neutron flux profiles and assembly power distributions in a slab reactor core. The results are comparable to those obtained from fine mesh diffusion theory calculations. The model is simple and can be easily implemented on a digital computer. In the fine mesh calculations, ten mesh points were located in each fuel assembly; the model required only one mesh point per assembly and thereby reduced the storage requirements on the computer.

The assumption that the flux in an assembly can be extended into the δ-regions of the surrounding assemblies and the use of empirical weighting factors to obtain the intra-nodal flux matching at the fuel assembly interfaces has proven to be very effective in simulating the fine mesh calculations. The use of an albedo boundary condition at the core-reflector interface is seen to be a very feasible substitute for the reflector nodes outside the reactor core.

The coarse mesh model described in this study was limited to a slab reactor core in one-dimensional geometry. The model can be easily extended to a quarter core geometry in two- and even three-dimensional geometry. This would only involve solving for more unknown coefficients in the polynomial representation for the flux in an assembly. The process of using empirical weighting factors to obtain flux matching can be extended to the higher-order dimensions also. It should be noted that the present study required a prior knowledge of the flux profiles to obtain the optimum weighting factors that yielded the best

agreement between the two calculations. Further study must be done to determine an analytical solution that will yield the optimum weighting factors directly. It should also be investigated if separate weighting factors apply to the fast and thermal fluxes. It is also suggested that an inner and outer iteration scheme be employed to improve the feedback between the assembly averaged flux calculations and the evaluation of the assembly polynomial coefficients.

Another area for further study is to determine a procedure to fit the correct albedo values at the core-reflector interface. Also, an adjustment for variations in the albedo value with coolant control poison concentration must be determined. It would also be desirable to simulate the effects of the core baffle by taking into account its effect on the albedo and flux profiles in the baffle region.

VIII. LITERATURE CITED

1. Borresen, S. 1971. A simplified, coarse mesh three dimensional diffusion scheme for calculating the gross power distribution in a BWR. Nuc. Sci. Eng. 44: 37-43.

2. Stout, R. B., and A. H. Robinson. 1974. Determination of optimum fuel loading in PWR using dynamic programming. Nucl. Tech. 24: 33.

3. Lin, Bo-in, B. Zolotar, and J. Weisman. 1979. An automated procedure for selection of optimal refueling policies for light water reactors. Nucl. Tech. 44: 258.

4. Chitkara, K., and J. Weisman. 1974. An equilibrium approach to optimal in-core fuel management for PWRs. Nucl. Tech. 24: 33.

5. Becker, M., and J. Celnik. 1971. Albedo models for nodal reactor simulation. Trans. Am. Nucl. Soc. 14: 832.

6. Steinke, Robert G. 1973. A coarse nodal method for solving the neutron diffusion equation. Ph.D. thesis. University of Michigan, Ann Arbor, Mi. 147 pp.

7. Graves, Harvey W., Jr. 1973. The evaluation of power distribution in large reactors using a two group nodal method. Ph.D. thesis. University of Michigan, Ann Arbor, Mi. 111 pp.

8. Delp, D. L., et al. 1964. FLARE — A three dimensional BWR simulator. USAEC Report GEAP-4598, General Electric Company, Atomic Power Equipment Department.

9. Pilat, E. E. 1971. CYREP-II: In-core fuel management code. NUS Corporation NUS-733.

10. Fenech, H. J., A. F. Rohach, et al. 1980. CYCLOPS: Advanced in-core fuel management optimization methodology for PWRs. EPRI Research Project RP 1251-1.

11. Adensam, E. G. 1969. Computer methods for utility reactor physics analysis. Reactor and Fuel Processing Tech. 12 (2): 225.

12. Ahlin, A., and M. Edenius. 1975. EPRI-CPM: The collision probability module. EPRI Research Project 118-1.

13. Duderstadt, James J., and Louis J. Hamilton. 1976. Nuclear Reactor Analysis. John Wiley and Sons, Inc., New York.

14. Rohach, A. F. 1979. DODMG: Diffusion theory, one dimensional multigroup diffusion program. Lecture notes. ISU NE 525.

IX. ACKNOWLEDGMENTS

The author gratefully acknowledges the kind assistance of Dr. Alfred E. Rohach in the pursuit of this study.

I wish to thank all my fellow degree candidates in the Nuclear Engineering Laboratory for their discussions — both technical and nontechnical. My special thanks are due to Mr. Sue Yih and Mr. Li-Wei Ho for their advice in the course of the computational calculations.

I also wish to thank the Department of Nuclear Engineering for providing assistance during the entire course of this study.

Finally, I wish to record the debt to my family for their constant encouragement and help.